Journal of Applied Polymer Science

Design and characterization of polypropylene matrix/glass fibers composite materials

Maria Sönmez,[1] Mihai Georgescu,[1] Mihaela Vâlsan,[1] Marius Radulescu,[2] Denisa Ficai,[2] Georgeta Voicu,[2] Anton Ficai,[2] Laurentia Alexandrescu[1]

[1]National Research & Development Institute for Textiles and Leather–division: Leather and Footwear Research Institute, Bucharest, Romania

[2]University POLITEHNICA of Bucharest, Faculty of Applied Chemistry and Material Science, 011061 Bucharest, Romania

Correspondence to: A. Ficai (E-mail: anton.ficai@upb.ro)

ABSTRACT: In this article, polymer composites based on polypropylene (PP) matrix reinforced with short glass fibers type E (GF-type E) were obtained. However, to ensure good interfacial adhesion and stress transfer across the interface, the influence of the chemical functionalization of the phases was analyzed. The better interfacial adhesion is assured by the use of maleic anhydride grafted PP and amino-functionalized GF. The obtained composite materials were tested from the point of view of composition, morphology, and mechanical properties. It can conclude that the chemical functionalization of the two phases is beneficial from the point of view of compatibility of the phases and consequently higher mechanical properties are obtained. © 2015 Wiley Periodicals, Inc. J. Appl. Polym. Sci. **2015**, *132*, 42163.

KEYWORDS: compatibilization; composites; mechanical properties; properties and characterization; surfaces and interfaces

Received 2 September 2014; accepted 1 March 2015

DOI: 10.1002/app.42163

INTRODUCTION

Continuous fiber reinforced thermoplastic (CFRT) composites offer new opportunities in the field of materials science. Products based on these materials can be processed to provide numerous physical properties tracked in the industry, such as report strength/weight high rigidity and high impact resistance and excellent fatigue resistance. These properties allow improved CFRT to be comparable to traditional structural materials such as aluminum and steel and consequently used in many industrial and medical applications with high mechanical loading.[1–5]

World's leading companies such as BASF,[6] Toyota,[7] and LANXESS[8] are doing researches related to the obtaining and even using composite polyamide, while Curv™ Composites[9] and Vetrorex[10] are studying polypropylene (PP) composites for automotive industry (protective bars, interior elements). The cooperation between GM, Basell Polyolefins, and Southern Clay leads to commercially available PP-based nanocomposite.[10]

These composite materials are obtained by mixing the polymer and reinforcing agents in specific equipment (mixers, rollers, extruders, etc.). For enhancing the adhesion between the phases, the reinforcing agent can be previously functionalized by using different functionalizing agents. The properties of the composite materials depend on the nature of polymer and reinforcing agent, the ratio between the phases, the used coupling agent, the dispersion rate, and the orientation of the fibers.[11–14] The size and morphology of the reinforcing agents are important for obtaining optimal properties of the composites.[14] The particle size of the fillers may vary within wide limits, from few nanometers in the case of silicon carbide to few tens of microns in the case of glass fibers (GF), for instance. The surface area is of major importance to the discontinuous phase dispersion in the polymer and the interactions at the interface polymer-reinforcing agent. The presence of the filler induces decreasing of the melt flow viscosity, increases the roughness and opacity of the composites, reduces the elasticity and abrasion resistance, and lowers the workability. Particle size distribution is also a very important feature because mechanical properties are strongly dependent on this.[15]

In order to improve adhesion between the matrix polymer and reinforcing agents, the most used methods is to modify the polymer or dispersed phase by using a third component known as "coupling agent". Silanes and titanates are the most used coupling agents and are used for the surface modification of the filler materials. Coupling agent or adhesion promoter is used to improve the adhesion (interaction) between the polymer and reinforcing agent (oxides, phosphates, silicates, etc.), as well as to withstand severe conditions of high temperature and

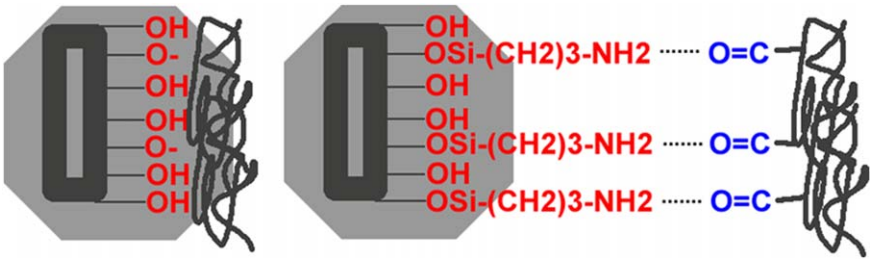

Figure 1. Schematic representation of the interactions between the two phases. [Color figure can be viewed in the online issue, which is available at wileyonlinelibrary.com.]

humidity.[16,17] Some of the most functionalization agents of the GF (silanes and titanates) as well as most used grafted polymers (PP-grafted-maleic anhydride or polyethylene-grafted-maleic anhydride[18–20]) are presented by Sonmez *et al.*[17] The compatibility between the two phases was recently studied for a lot of binary systems, including green composites.[17,19,21–25] In fact, the properties of these composites are strongly dependent on nature and relative ratio of the components, processing route as well as the used compatibilization agents. Usually, the properties of the composites are enhanced by functionalizing the filler with adequate agents. The functionalizing agents present at least two moieties, one able to bind to the filler (silane groups are most probably the most known and used such moiety) while the other moiety is mainly responsible with improving the compatibility with the polymer matrix.[17,26,27] These grafted polymers are cheap and have found a fairly wide applicability in obtaining Polymer Matrix Composites.[17,21,22,28]

(3-aminopropyl)trimethoxysilane (APTMS) is widely used for the functionalization of a wide variety of silica-based materials because silica-based materials (silica and silicates, mesoporous silica and zeolites, glass, etc.) present a lot of silanol groups (Si–OH) which impose an hydrophilic surface. In the case of polyolefin matrix composite materials, the hydrophobic polyolefin have limited of no interaction with the silica-based materials and consequently agglomerations appear and mechanical properties are decreasing. For these purposes, before compounding with polyolefins, GF can be modified by using APTMS.[17]

In this article, polymer composites based on PP mixed with 1 or 3% PP-*g*-MA and various proportions of short GF-type E treated with APTMS were obtained. Owing to the low interaction/compatibility of the two phases (hydrophobic nature of PP and hydrophilic nature of GF-type E), the surface of the GF-type E was chemically modified by using APTMS (APTMS-GF-type E) while the PP was modified in bulk with maleic anhydride (the GF-type E surface is enriched in amino groups which can interact with the anhydride groups of PP by hydrogen bonds) (Figure 1). The main purpose of the functionalization is related to the necessity of improving the compatibility of the two phases (hydrophobic PP and hydrophilic glass surface). For this reason, the GF are treated with APTMS leading to amine functionalized glass surface while 1 or 3% PP-g-MA were used as a secondary compatibilizer. This technology was also used for the obtaining of PP/clay nanocomposites.[29] The interactions between the phases will be further discussed in the section titled "FTIR Spectroscopy and Microscopy".

EXPERIMENTAL

Untreated borosilicatic GF-type E ($L = 4.5$ mm, $d = 13\mu$m, Camelyaf Glass), (3-aminopropyl)trimethoxysilane (APTMS 97%, Sigma-Aldrich), isotactic PP (PP Impact copolymer TIPPLEN K 948, Tiszai Vegyi Kombinat RT (TVK), Hungary), PP grafted with maleic anhydride (Sigma-Aldrich, USA, MW ~ 9100, average Mn ~ 3900, maleic anhydride content 8–10 wt %) were used without any further processing.

Functionalization of Glass Fibers

The functionalization of GF-type E was done by spraying aqueous solution of APTMS (5%) onto the GF followed by drying at room temperature for 24 h and finally heating at 80°C, overnight (APTMS-GF-type E). The amount of APTMS was 5% reported to GF.[17] The GF functionalization consists in partial or fully transformation of Si–OH groups in Si–OR ester groups.

Preparation of PP/APTMS-GF-Type E Composite Materials

Six composite materials were obtaining starting from PP mixed with 1 or 3% PP grafted with maleic anhydride and APTMS-GF-type E, as result from Figure 2. For having additional reference materials, two additional standard specimens were obtained, meaning FS2* = P2* and FS6* = P6*. In these cases, bare GF-type E and no PP-*g*-MA was used.

Table I presents the content of the two types of composite materials. In all cases, the homogenization was achieved in a TSE35 co-rotating twin screw extruder granulator. The two types of materials mainly differ due to the content of PP-*g*-MA, the samples denoted with P contain 1% of PP-*g*-MA while the samples denoted with FS contain 3% of PP-*g*-MA. The sample denoted with PP corresponds to pure PP (without any PP-*g*-MA). The content of APTMS-GF-type E is presented in Table I.

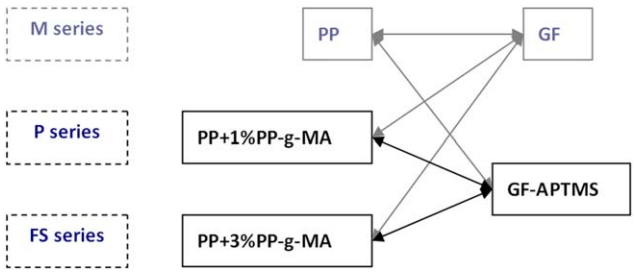

Figure 2. Design of composite materials. [Color figure can be viewed in the online issue, which is available at wileyonlinelibrary.com.]

Table I. The Composition of the Two Types of Receipts

The receipt code	PP	P0	P1	P2	P3	P4	P5	P6
Content of silanized GF, %	0	0	5	10	15	20	25	30
PP-*g*-MA content, %	0	1	1	1	1	1	1	1

The receipt code	PP	FS0	FS1	FS2	FS3	FS4	FS5	FS6
Content of silanized GF, %	0	0	5	10	15	20	25	30
PP-*g*-MA content, %	0	3	3	3	3	3	3	3

Achieving Standard Specimens for Mechanical Testing

Standard specimens (Figure 3; Table II) were obtained in order to determine the physicomechanical indicators by using a laboratory electric press FONTIJNE GROTNES BV. For this reason, 70 g of granules obtained from the twin screw extruder were placed in a forming mould of l50 × l50 × 2 mm and processed in the electric press. Three main steps can be identified:

- Preheating for 10 min at a temperature of 165°C and a pressure of 150 kN.
- Pressing for 12 min at a temperature of 165°C and a pressure of 300 kN.
- Cooling down to 35°C at a pressure of 300 kN—this step takes 12 min.

Quality Control of the P and FS Standard Specimens

Prior to testing, all the samples are conditioned for 24 h at room temperature. The quality control of the obtained samples involves the determination of the following characteristics/properties:

- Physicomechanical properties (tensile strength and hardness) were determined according to the standard in force for plastics reinforced with GF. The standard specifies a method for determining the tensile characteristics of fiber-reinforced plastics bottle.
- Traction unit effort is the traction, supported by the specimen in every moment of the attempt, per unit area of the initial straight section calibrated portion of the specimen.
- Composition
- Morphology
- Melt flow index.

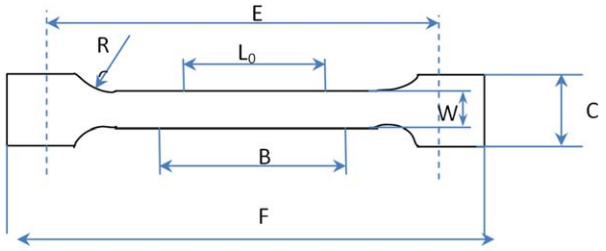

Figure 3. Dumbbell type specimen used for mechanical testing. [Color figure can be viewed in the online issue, which is available at wileyonlinelibrary.com.]

Melt flow index was determined by using a HAAKE MELTFIX 2000 equipment. Because the melt index depends on the nature and hardness of the composite materials as well as the applied force, all samples were analyzed by applying a 5 kg force and an operating temperature of 180°C, while all the other parameters being kept constant.

Three values were derived including volumetric flow index values (MVR, cm^3/10 min), value of the mass flow (MFR, g/10 min), and the average of the two indices.

Polymer composites reinforced with functionalized GF were morphologically and structurally characterized by X-ray diffraction (XRD), infrared spectroscopy (FT-IR), and scanning electron microscopy (SEM).

The composite materials were characterized by FTIR spectroscopy, XRD, and SEM. FTIR data were obtained by using a Thermo iN10 MX FT-IR microscope operated in reflection mode. All the spectra were obtained in reflection mode, using a cooled imaging detector (MCT Array) by co-adding 16 spectra at a spectral resolution of 8 cm^{-1} while the time of acquisition was 3 s/scan.

XRD analysis was performed using a Shimadzu XRD 6000 diffractometer at room temperature. In all the cases, Cu-K_α radiation from a Cu X-ray tube (run at 15 mA and 30 kV) was used. The samples were scanned in the Bragg angle, 2θ range of 10–80°, with a sampling interval of 0.02.

SEM images were recorded on a HITACHI S2600N scanning electron microscope. Prior to analysis, all samples were coated with a thin layer of silver to improve conductivity using a home-made sputtering system.

Table II. Characteristics of Specimens Made of Glass Fiber Thermoplastics

Characteristics	Symbol	Type I
Overall length, min	F	150
Width extremities (ends)	C	20 ± 0.5
Thickness	H	1-10
Length of the calibrated	B	60 ± 0.5
Width of calibrated	W	10 ± 0.5
Reference length	L_0	50 ± 0.5
The distance between the clamps	E	115 ± 5

Table III. Physicomechanical Characterization of the Polypropylene Composites Reinforced with Glass Fibers Treated in the Presence of 1% PP-*g*-MA

The receipt code	PP	P0	P1	P2[a]	P2	P3	**P4**	P5	P6[a]	P6
GF content	0	0	5	10[a]	10	15	**20**	25	30[a]	30
Physicomechanical characterization										
Tensile strength (N/mm^2)	6.21	6.51	12.4	18	25	37	**50**	22	11	11
Hardness (°Sh D)	70	69	71	65	72	74	**77**	80	70	83

[a] Px is similar with the sample Px but no PP-g-MA is used (*FSx = *Px).

RESULTS AND DISCUSSION

Mechanical Properties of Composite Materials

For this reason, hardness and tensile strength were determined. The experiments were carried out without adding GF to the matrix as well as by varying the quantity of GF in a percentage of 5, 10, 15, 20, 25, and 30% and by varying the coupling agent PP-*g*-MA at a rate of 1–3% (used to improve the compatibility dispersed phase polymer matrix and reduce the viscosity of the mixture). The values obtained were compared with the control sample containing no GF. The results are shown in the Tables III, IV and Figure 5.

The **hardness values** vary appreciable proportional with the content of reinforcing agent, from 69 to 83°Sh D for the samples P0–P6 and from 67 to 72°Sh D for the samples FS0–FS6. It can be observed that for the sample P0 (the reference sample containing only PP and 1% PP-*g*-MA), the hardness decreases slightly compared to the reference PP with only 1°Sh D. The same finding can be observed for the sample FS0 (the reference sample containing only PP and 3% PP-*g*-MA) but, in this case, the decreases is of 3°Sh D (from 70 to 67°Sh D). It is also evident that the hardness increases with increasing the content of GF for the composite samples P1–P6 (71–83°Sh D) as well as for the composite samples FS1–FS6 (69–72°Sh D). However, it is observed that increasing the proportion of 3% coupling agent significantly reduces the hardness of the mixture even at the same concentrations of GF, which demonstrates that the PP grafted with maleic anhydride has a double role: plasticizer—reducing the viscosity of the mixture—and coupling agent.[23,25] The workability of the composite is also improved due to lower melt viscosity as well as homogenous dispersion of GF polymer mass. The variation of the hardness of the samples is presented in Figure 4. The hardness of P2* (=FS2*) drastically decrease comparing with the PP sample as well as comparing with the P and FS series. The explanation of this decreasing hardness can be attributed to the low interactions between the phases. This low compatibility between the phases leads to voids between the PP matrix and GF-type E. In the case of P6*(=FS6*), the hardness is even lower because of the higher microstructural heterogeneity induced by the addition of 30 wt % bare GF-type E, which leads to voids and crack and an overall decrease of the mechanical properties of the composites.

The **tensile strength** of the polymer composites shows major variations comparing with pure PP being dependent on the content of PP-*g*-MA as well as the content of reinforcing agent. The increase of the content of PP-*g*-MA from 0% in the case of pure PP to 1% in the case of P0 leads to an insignificant increase of the tensile strength from 6.21 to 6.51 N/mm^2 but, when the content of PP-*g*-MA increases to 3%, the tensile strength became 11 N/mm^2. So, based on these data, we can conclude that 3% PP-*g*-MA leads to an improvement of this property.

In the case of the samples P0–P4, we can observe a significant increase of the tensile strength value from 6.51 to 50 N/mm^2. This demonstrates the strong interactions between the aminopropyl groups of the functionalization agent and the used PP-*g*-MA (also maleic ring opening can occur under the influence of temperature and torsion forces[30]) and therefore better adhesion between the reinforcing agent and polymer matrix due to the formation of strong hydrogen bonds. The use of the APTMS-GF-type E leads to a stuffing hydrophobic and organophilic surface of the GF that leads to optimal compatibility with the organic polymer. The positive effects of the simultaneous use of PP-g-MA and APTMS-GF-type E can be easily proved by comparing the tensile strength of P0–P6 and FS0–FS6 with the PP-GF-type E (0–30%). For this purpose, two reference standard specimens based on PP and 10% and 30% of bare GF-type E were obtained and tested similarly with the FSx and Px series. It can be seen that the tensile strengths of both standardized specimens obtained from PP and bare GF-type E are much lower than that of the Px and FSx series. As expected, the lowest tensile strength corresponds to the sample #6 (P6* = FS6* because no PP-*g*-MA was used) because of the high content of GF-type E and the low compatibility between the phases. In the case of mixtures P5 and P6, the tensile strength decreases down to 22

Table IV. Physicomechanical Characterization of the Polypropylene Composites Reinforced with Glass Fibers Treated in the Presence of 3% PP-*g*-MA

The receipt code	PP	FS0	FS1	FS2[a]	FS2	FS3	FS4	**FS5**	FS6[a]	FS6
GF content	0	0	5	10[a]	10	15	20	**25**	30[a]	30
Physicomechanical characterization										
Tensile strength (N/mm^2)	6.21	11	19	18	33	42	50	**60**	11	29
Hardness (°Sh D)	70	67	69	65	70	71	71	**71**	70	72

[a] FSx is similar with the sample FSx but no PP-g-MA is used (*FSx = *Px).

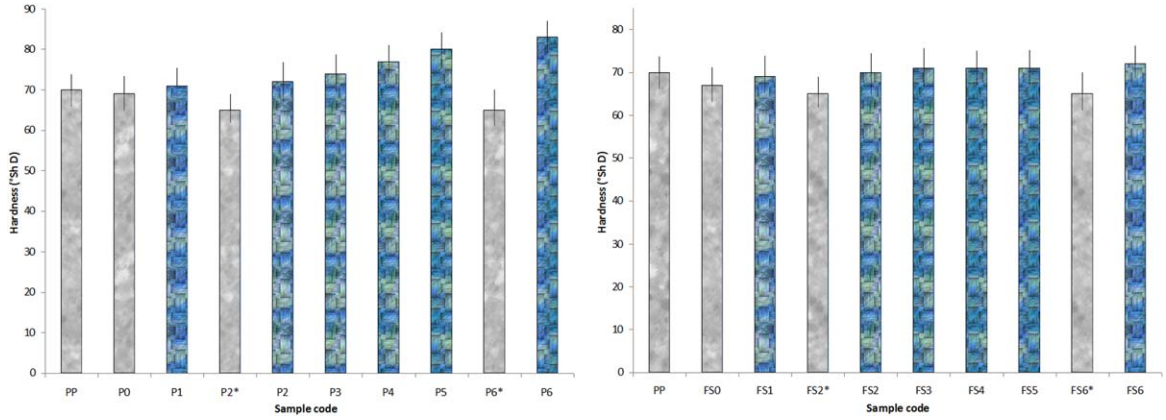

Figure 4. The variation of the hardness of the samples function of the composition. [Color figure can be viewed in the online issue, which is available at wileyonlinelibrary.com.]

and then to 11 N/mm^2 once the content of GF increases to 25 and 30%. This is because the viscosity of the mixture increases and consequently decreases the ability of the polymer to wet all fiber glass properly leading to agglomeration, which represents the emergence defects in the material and lead to the break of the specimens. In the case of composite materials containing 3% PP-*g*-MA, a larger increase is observed in comparison with the tensile strength obtained for the samples P1–P6 (containing 1% PP-*g*-MA), even at the same percentage of GF.

The tensile strength of the composite materials obtained with 3% PP-*g*-MA (FS0–FS5) increases with increasing the amount of APTMS-GF-type E from 11 to 60 N/mm^2, which demonstrates that increasing concentration of PP-*g*-MA is acting as an internal lubricant lowering the viscosity of the composition. Also, the chain structure of the silane coupling agent can interpenetrate with the PP-*g*-MA molecules leading to improved tensile resistance. At high concentrations of APTMS-GF-type E 30%, for composite FS6, we can observe a strong decrease of the tensile strength (down to 29 N/mm^2), most probably due to the excess of GF which cannot develop supplementary hydrogen bond with the PP-*g*-MA. Comparing the two types of materials, it can be concluded that increasing content of PP-*g*-MA allows a higher filler uptake. This can be easily explained tacking into account the higher carbonyl centers and consequently the number of hydrogen bonds with APTMS-GF-type E. Usually, the best mechanical properties are obtained for certain volumetric ratio, this ratio being dependent of many factors: specific surface area of the filler, processing route, temperature of blending, and so on. But in the case of many fiber-reinforced PP materials, the optimal content of fibers is usually <30–40%.[31] Based on our results, the mechanical properties increase up to ~50 vol % (meaning 25 wt %) which means that this compatibilization procedure is very efficient.

Determination of the Melt Flow Index of the Polymer Composites Obtained

The melt flow indices provide information on the nature of the material such as the degree of pushing or laminates and temperature degradation. The thermoplastic composites may be determined by testing the influence of variations in temperature and/or the weight values of pressure–flow index (MFI). The density and melt flow index values of the P and FS samples are shown in Tables V and VI.

According to Tables V and VI, it is observed that the flow rate and density of the polymer composites tested are influenced by the amount of reinforcing/agent and the amount of PP-*g*-MA.

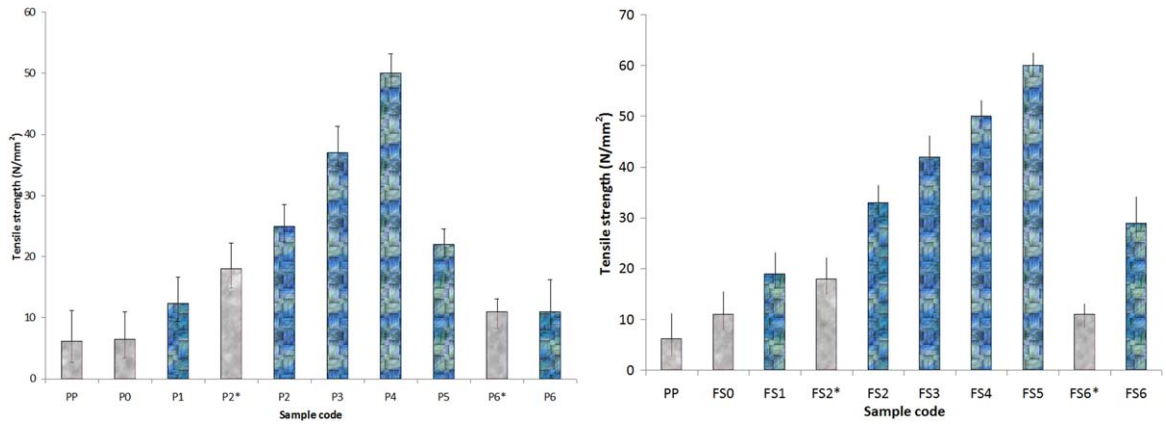

Figure 5. Tensile strength variation depending on the content of APTMS-GF-type E. [Color figure can be viewed in the online issue, which is available at wileyonlinelibrary.com.]

Table V. Density and Specific Flow Index Values of Composites Based on Polypropylene/PP-*g*-MA 1%/Glass Fibers Treated with 3-APTMS

Sample code	Density (g/cm^3)	MVR (cm^3/10 min)	MFR (g/10 min)
PP	0.90	118	113
P0	0.93	104	96.3
P1	0.96	86.4	83.0
P2	0.97	46.6	47.5
P3	1.02	44.9	47.4
P4	1.04	44.8	46.7
P5	1.04	44.1	42.8
P6	1.06	38.8	40.3

In addition, it can be noticed that the values of fluidity and densities decrease with increasing surface coupling agent represented by PP-*g*-MA and increased proportionally with the increase of proportion of reinforcement or reinforcing agent.

The melting indices of the thermoplastic composite materials, MVR and MFR, depend on the shear rate. In these tests, shear velocities are much lower than in normal conditions of processing into finished products.

The two indices decrease with increasing the content of reinforcing agent except the case of FS0. This anomaly can be explained taking into account that once with the increasing of the content of GF, the viscosity increases and, theoretically MVR and MFR decrease. In the case of FS0, the viscosity decreases because of the strong interactions between GF. The analysis of the melt flow index values of the composite materials based on PP mixed with 1 or 3% PP-*g*-MA reinforced with functionalized GF may be used for determining the processing parameters into finished products by injection molding. Based on these data, the following parameters can be determined:

1. Injection temperature—180°C.
2. Injection time—3 min.
3. Pressure injection—5 atm.
4. Auger rotation speed—180 rev/min.

Table VI. Density and Specific Flow Index Values of Composites Based on Polypropylene/PP-*g*-MA 3%/Glass Fibers Treated with 3-APTMS

Sample code	Density (g/cm^3)	MVR (cm^3/10 min)	MFR (g/10 min)
PP	0.90	118	113
FS0	0.93	137	127
FS1	0.98	89.5	87.7
FS2	1.03	63.1	67.5
FS3	1.06	49.5	52.5
FS4	1.07	48.5	51.4
FS5	1.07	41.0	43.9
FS6	1.09	38.7	42.2

Compositional and Morphological Characterization of Composite Materials

The materials obtained are characterized in terms of morphological and microstructural behavior and the characterization was done by SEM and FTIR microscopy. Also, FTIR microscopy can reveal morphological and compositional aspects, by selecting the desired wavelength.

Scanning Electron Microscopy

The obtained composite materials were characterized in terms of the microstructure. Four types of composite materials were comparatively analyzed, all the images being recorded in the fracture resulted during the mechanical testing. The first analyzed sample corresponded to PP/GF-type E, the second to PP/APTMS-GF-type E while the last two samples to the PP+1% PP-*g*-MA/APTMS-GF-type E (P6) and PP+3% PP-*g*-MA/APTMS-GF-type E (FS6) samples, respectively. In all cases, the reinforcing agent comprises 30% of the final composite material. One can observe significant differences between the samples of composite materials based on PP and GF. The different morphology is given by the content of PP-*g*-MA (0, 1, and 3%) as well as the functionalization of the GF. If using 3% PP-*g*-MA, the compatibility between the phases is optimum; virtually all GF are fully coated with polymer phase. In the case of P6 sample, the compatibility is limited due to the low content of MA. In the case of PP/APTMS-GF-type E, only limited compatibilization of the phases is granted. In the case of PP/GF, the compatibilization is the worst and practically no polymer can be seen on the GF surface. Based on this, we can say that functionalization of GF and maleic anhydride grafting lead to better compatibility between phases. Etcheverry and Barbosa[25] used SEM to analyze the fracture section of different PP/GF samples. Visual observation of the surface of the GF reported by Etchevery *et al.* is very similar with the images from Figure 6a–c, especialy with the SEM images recorded on the P series (in the figure only P6 is presented) or the samples PP-APTMS-type E presented in our previous work.[17] The radial matrix crack developed during fragmentation indicates a good matrix fiber adhesion for all samples, especially for the FS6. In this case, the polymer phase is so well anchored that practically polymer does not detach from the GF.

FTIR Spectroscopy and Microscopy

Composite materials based on PP and GF have also been characterized by FTIR spectroscopy and microscopy. The FTIR spectral characterization can be done easily especially based on the existent literature data.[17] FTIR spectra of the FS6 (Figure 7) exhibit the characteristic peaks of the components. The presence of the isotactic PP can be visualized based on the peaks 2950 (asymmetric CH_3 stretching vibration), 2918 (asymmetric CH_2 stretching vibration), 2867 (symmetric CH_3 stretching vibration), 2840 (symmetric CH_2 stretching vibration), 1455 (is due to the overlapping of the asymmetric bending mode of the methyl (CH3) and the methylene (CH_2) scissoring mode), 1375 (symmetric CH_3 deformation), and 716 cm^{-1} (rocking vibrations of methylene groups[32]). The bands from around 1375 and 1450 cm^{-1} are usually monitored for studying the interactions between the phases (PP and glass/functionalized GF).[33] Even not presented in Figure 7 (due to high number of samples), the

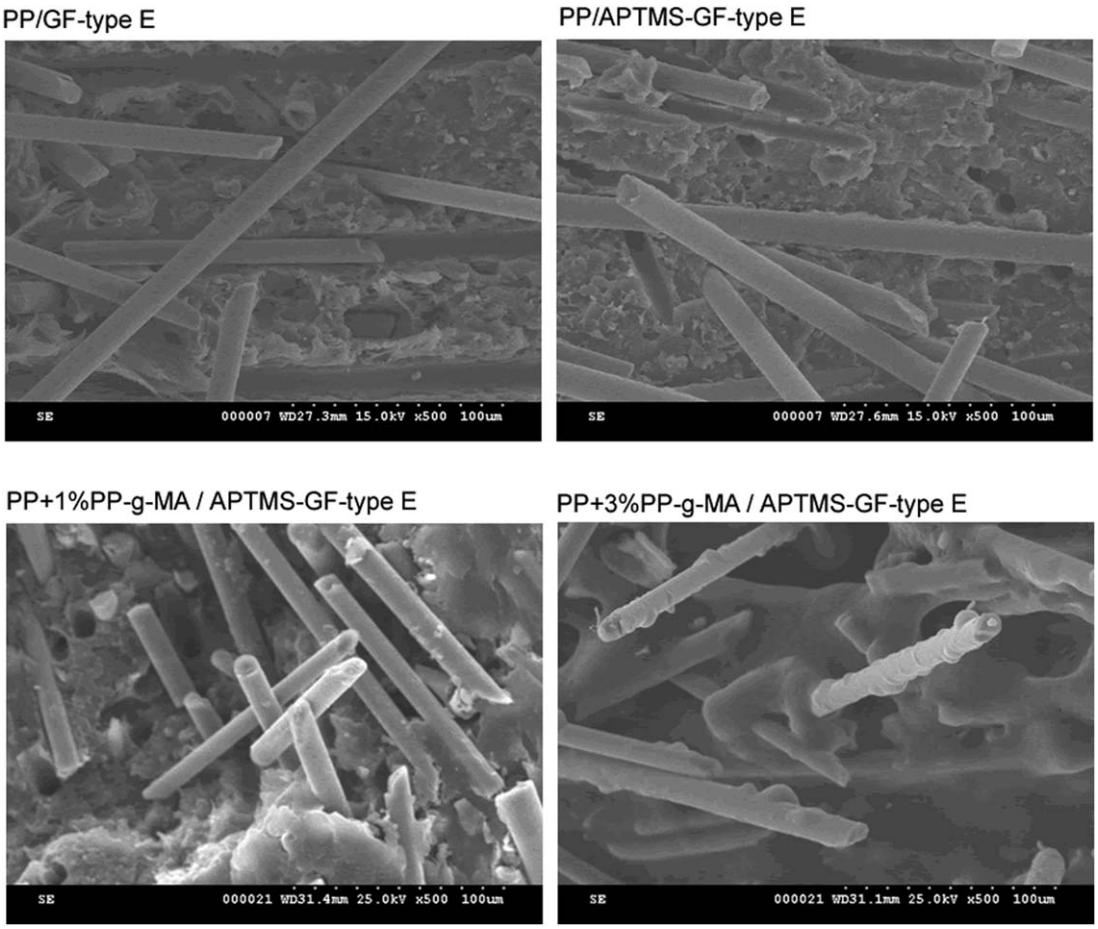

Figure 6. Characteristic SEM images of PP based composite materials reinforced with GF-type E (a) or with 30% APTMS-GF-type E (b-d) at 500x magnification.

slight shift of these bands prove the increasing of the interactions between the phases, especially in the case of FS5 (which proved the best mechanical properties). The peaks from 1166 or 1752 cm^{-1} are indicating the presence of the isopropyl group belonging to the reinforcing agent—APTMS-GF-type E (see also the spectrum of APTMS-GF-type E). Even if the bands from 1160, 997, 973, and 841 cm^{-1} are less intense, their analysis must be done because they are correlated with the tacticity of

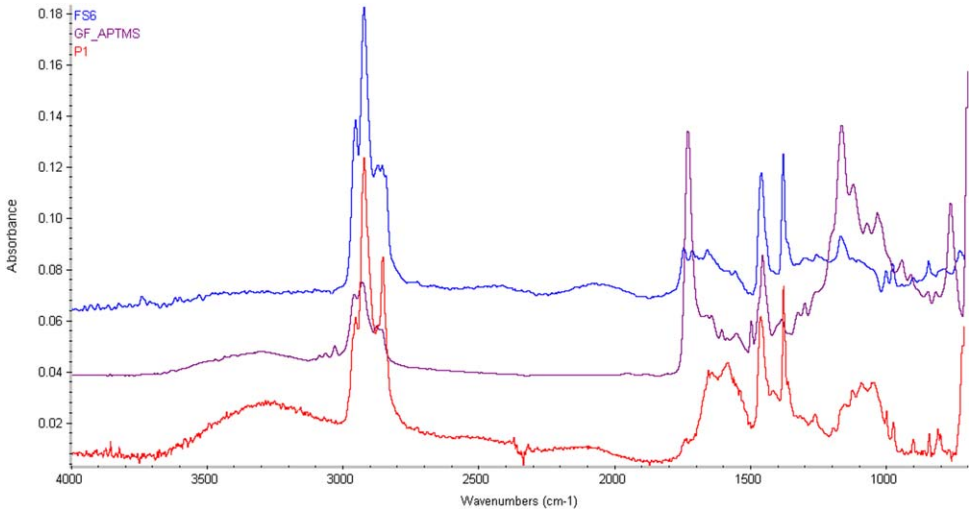

Figure 7. FTIR spectra of APTMS-GF, P1 (PP+1% PP-*g*-MA/5%GF type E-APTMS) and FS6 (PP+3% PP-*g*-MA/30% APTMS - GF-type E). [Color figure can be viewed in the online issue, which is available at wileyonlinelibrary.com.]

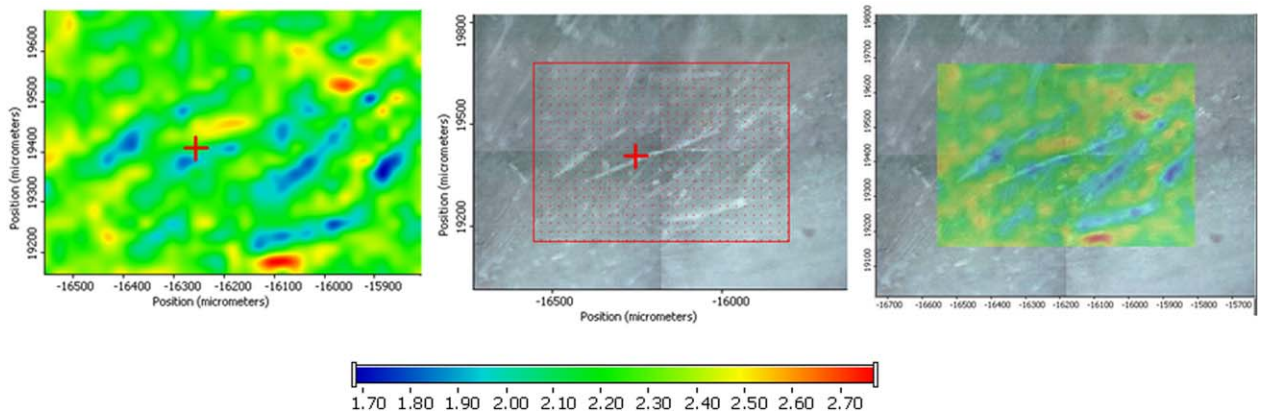

Figure 8. FTIR images for the sample P6, in cross-section monitored at 2950 cm^{-1}. [Color figure can be viewed in the online issue, which is available at wileyonlinelibrary.com.]

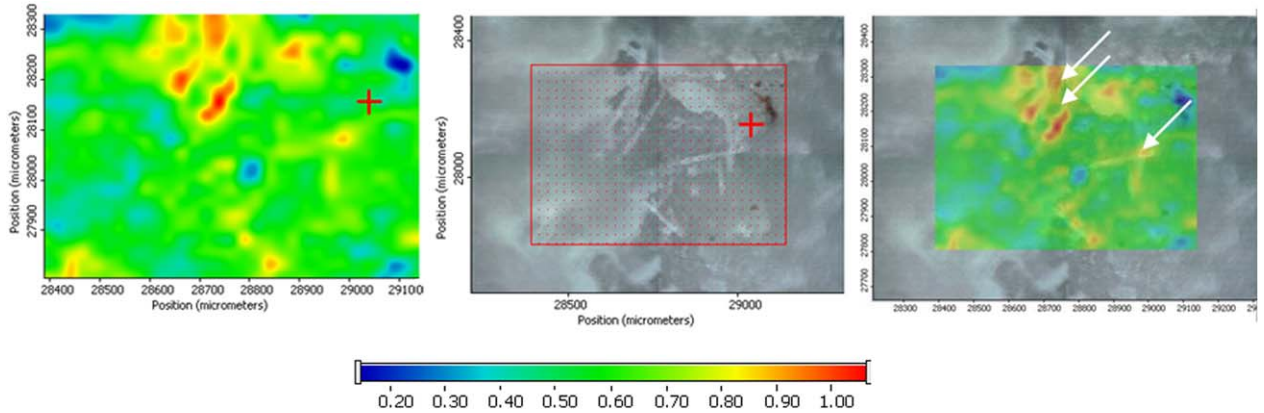

Figure 9. FTIR images for the sample FS6, in cross-section monitored at 2950 cm^{-1}. [Color figure can be viewed in the online issue, which is available at wileyonlinelibrary.com.]

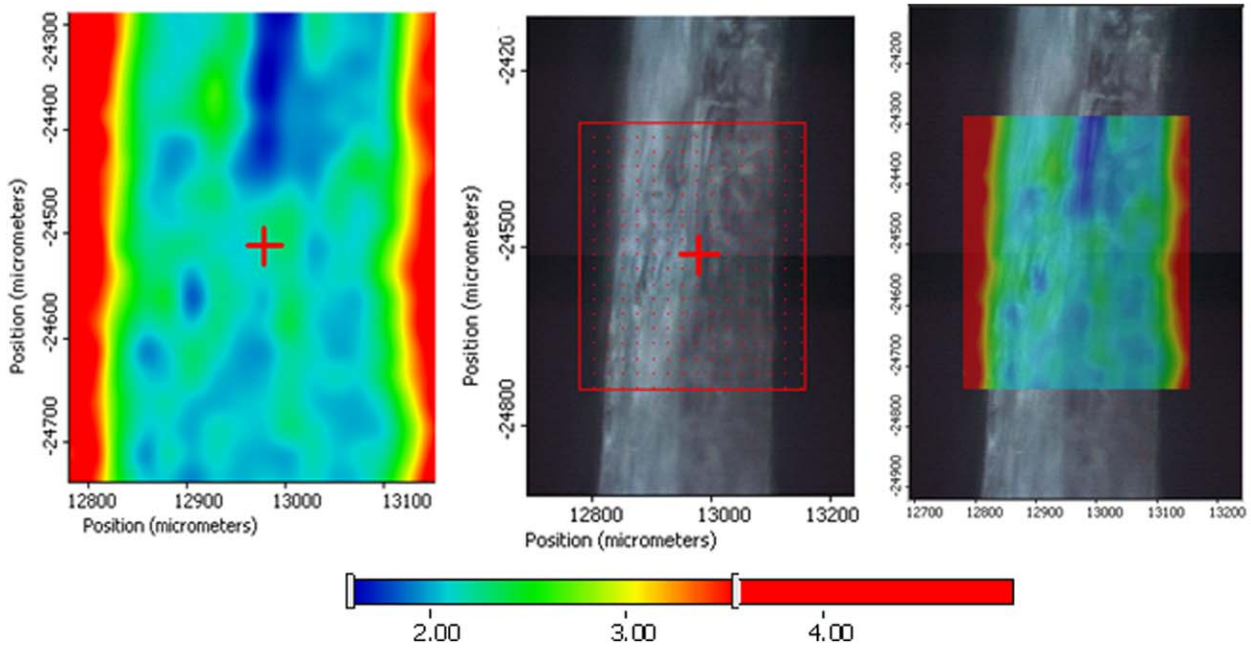

Figure 10. FTIR characteristic images of thin P1 sample, in cross-section, at 2950 cm^{-1}. [Color figure can be viewed in the online issue, which is available at wileyonlinelibrary.com.]

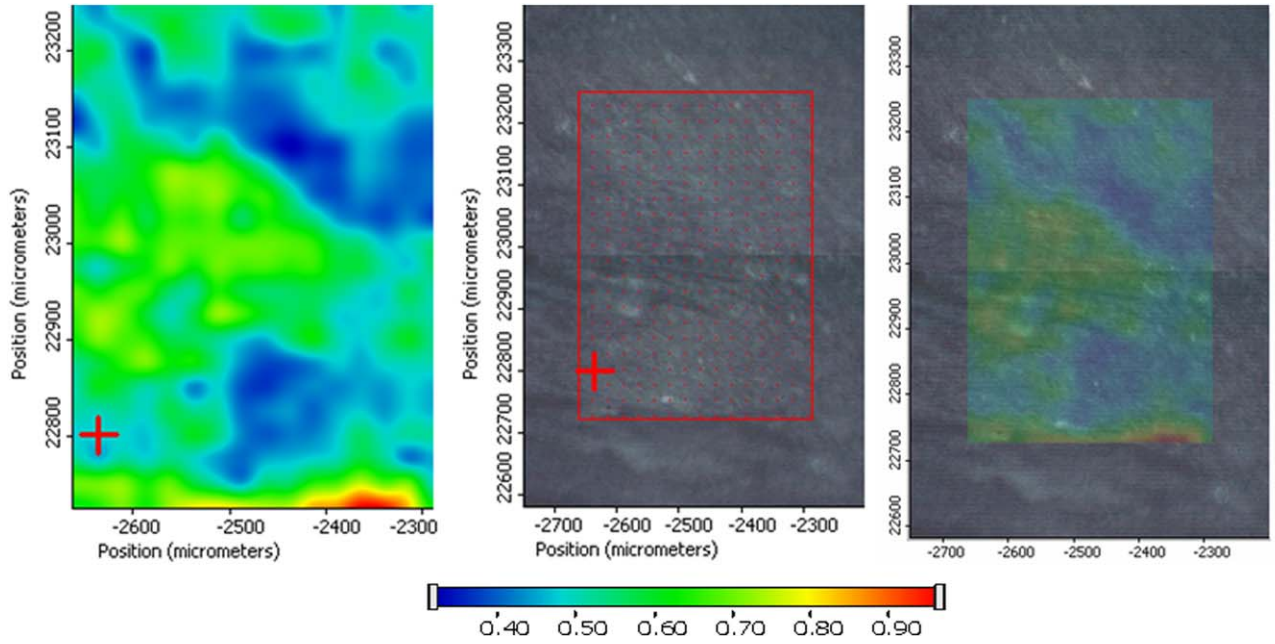

Figure 11. FTIR characteristic images of PP sample, in cross-section, at 2950 cm^{-1}. [Color figure can be viewed in the online issue, which is available at wileyonlinelibrary.com.]

the polymer.[32] The presence of the PP-*g*-MA can be easily monitored based on the specific peaks between 1500 and 1700 cm^{-1}.

It is worth to mention that the composite sample (see the FTIR spectrum of PP+3%PP-*g*-MA/ APTMS-GF-type E) exhibits no broad band at 3000–3500cm^{-1} which means that no associated groups are present (neither hydroxyl nor amino groups) even if, in the case of silanized GF, their presence is obvious. Also the peak form 1736 cm^{-1} is strongly shifted, and this can be explained based on the strong interactions between the anhydride and amino groups, similar shifts being observed in many different composite materials.[34]

In this regard, monitoring was performed at a wavelength characteristic of the component of interest. Regardless of the test sample can highlight GF embedded in the polymer matrix.

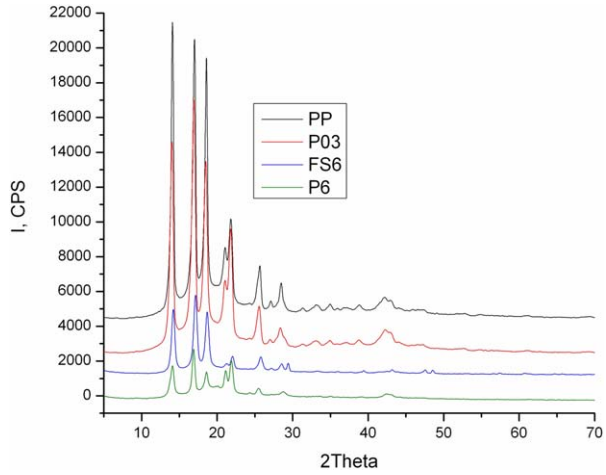

Figure 12. The X-ray diffractograms of the sample PP, P03, P6, and FS6. [Color figure can be viewed in the online issue, which is available at wileyonlinelibrary.com.]

The FTIR microscopy obtained at 2950 cm^{-1} reveals characteristic images of the sample P6 (PP+1% PP-*g*-MA/APTMS-GF-type E—Figure 8). Thus, the regions reached in APTMS-GF-type E contain low level of PP and PP-*g*-MA, as we can conclude from the quantitative distribution of the PP and GF, based on the data obtained at 2950 cm^{-1}.

In the case of P6 sample (similar to FS6 but containing 3% PP-*g*-MA), at the first look, the data seems to be strange because the intensity of the PP is very high on the surface of the GF (Figure 9—marked with arrows). This can be easily explained, especially if we corroborate these data with the SEM images, from where, it can be clearly concluded that PP intimately cover/embed the GF.

FTIR microscopy can also be used for the determination of the overall morphology of the composite sample. For instance, in the case of thin P1 sample, based on the cross-section FTIR image, we can determine the thickness of the sample (300 μm) and the homogeneity of the sample (this sample due to the low content of filler (5%) has more homogeneous morphology comparing with the above analyzed samples (FS6 and P6, both containing 30% filler), practically no fibers can be identified on the surface (Figures 10 and 11).

The FTIR micrograph of the pure PP reveals a smooth fracture surface and limited or no heterogeneity, the color change being a result of the hill-valley morphology of the fracture.

XRD Diffraction

The obtained composite materials were characterized from the point of view of the existing crystalline phase (Figure 12). One can see that the commercial isotactic PP is highly crystalline

and the crystallinity decreases once with the addition of GF and PP-*g*-MA. The lowest crystallinity is observed for the sample FS6 which contain the highest amount of GF (30%) and the highest amount of PP-*g*-MA (3%).

CONCLUSIONS

In this article, polymer composites based on PP and short GF-type E were obtained. The compatibilization of the two phases was achieved by treating GF with APTMS while the polymer matrix was blended with 1 or 3% of PP-*g*-MA. The compatibility of the two phases increases very much as supported by our data. Based on the SEM images, the original PP/GF-type E composite material presents no interfacial adhesion. The best adhesion occurs in the case of FS5 (containing 25% APTMS-GF-type E) because the functionalization of both matrix and reinforcing agent happens with the introduction of reactive groups between which very strong hydrogen bonds can develop. The better compatibility of the phases also induces an increasing of the mechanical properties of these samples.

ACKNOWLEDGMENTS

The financial support of the PNII-PT-PCCA-2011-3.2–1392 "Hybrid Composite Materials with Thermoplastic Matrices Doped with Fibers and Disperse Nano Fillings for Materials with Special Purposes - HybridMat" supported by the Romanian Ministry of Education is gratefully acknowledged.

REFERENCES

1. Spiegel, J. Development of continuous fibre reinforced nylon composites for structural applications-Polystrand Company, In: 12th Annual Automotive Composites Conference & Exhibition, MSU Management Education Center811 W. Square Lake Road Troy, MI, **2012**.
2. van Heumen, C. C. M.; Kreulen, C. M.; Bronkhorst, E. M.; Lesaffre, E.; Creugers, N. H. *J. Dent. Mater.* **2008**, *24*, 1435.
3. Matsuki, T.; Yamaguchi, T.; Matsushita, H.; Niwa, K.; Fujita, K. *Int. Sampe. Tech. Conf.* **1991**, *36*, 582.
4. Fisher, E. H.; Gibson, A. G. *Plast. Rub. Compos. Pro.* **1998**, *27*, 447.
5. Wongsriraksa, P.; Togashi, K.; Nakai, A.; Hamada, H. *Adv. Mech. Eng.* **2013**, 6, http://dx.doi.org/10.1155/2013/685104.
6. BASF Explores Nylon Composites for Cars, in: Plastic Technology, http://www.ptonline.com/articles/basf-explores-nylon-composites-for-cars, **2012**.
7. .U. A., Nylon 6-Clay Hybrid. R&D Review of Toyota CRDL: Technology Public Relations Sec. Intellectural Property Div. TOYOTA CENTRAL R&D LABS. INC., 2005.
8. .Front end produced by hybrid technology with nylon composite sheet – Technical Information, in: vol 2014, LANXESS Deutschland GmbH, 2010.
9. Jones, R. S.; Riley, D. E. A new self-reinforced polypropylene composite, in: 2nd Annual Automotive Composites Conference & Exhibition2012, MSU Management Education Center811 W. Square Lake Road Troy, MI.
10. Flowers, B., Ed. Automotive Applications for Polypropylene and Polypropylene Composites; Marcel Dekker, Inc.: New York, **2009**.
11. Nath, D. C. D.; Bandyopadhyay, S.; Yu, A. B.; Blackburn, D.; White, C. **2010**, *45*, 1354.
12. Ficai, A.; Andronescu, E.; Voicu, G.; Ghitulica, C.; Vasile, B. S.; Ficai, D.; Trandafir, A. *Chem. Eng. J.* **2010**, *160*, 794.
13. Andersons, J.; Joffe, R. *Compos. A Appl. S.* **2011**, *42*, 1229.
14. Roeder, R. K.; Converse, G. L.; Kane, R. J.; Yue, W. *JOM*, **2008**, *60*, 38.
15. Pramanik, N.; Mohapatra, S.; Alam, S.; Pramanik, P. *Polym. Compos.* **2008**, *29*, 429.
16. Navarro-Banon, V.; Vega-Baudrit, J.; Vazquez, P.; Martin-Martinez, J. M. *Macromol. Symp.* **2005**, *221*, 1.
17. Sonmez, M.; Ficai, D.; Ficai, A.; Alexandrescu, L.; Voicu, G.; Andronescu, E. *Rev. Rom. Mater.* **2014**, *44*, 88.
18. Del Castillo-Castro, T.; Castillo-Ortega, M. M.; Herrera-Franco, P. J.; Rodriguez-Felix, D. E. *J. Appl. Polym. Sci.* **2011**, *119*, 2895.
19. Martinez-Colunga, J. G.; Sanchez-Valdes, S.; Ramos-deValle, L. F.; Munoz-Jimenez, L.; Ramirez-Vargas, E.; Ibarra-Alonso, M. C.; Lozano-Ramirez, T.; Lafleur, P. G. *J. Appl. Polym. Sci.* **2014**, 131.
20. Zhou, J. S.; Yan, F. Y. *J. Appl. Polym. Sci.* **2004**, *93*, 948.
21. Srubar, W. V.; Pilla, S.; Wright, Z. C.; Ryan, C. A.; Greene, J. P.; Frank, C. W.; Billington, S. L. *Compos. Sci. Technol.* **2012**, *72*, 708.
22. Avolio, R.; Gentile, G.; Avella, M.; Carfagna, C.; Errico, M. E. *Eur. Polym. J.* **2013**, *49*, 419.
23. Sobczak, L.; Bruggemann, O.; Putz, R. F. *J. Appl. Polym. Sci.* **2013**, *127*, 1.
24. Hemmati, F.; Garmabi, H.; Modarress, H. *Polymer* **2014**, *55*, 6623.
25. Etcheverry, M.; Barbosa, S. E. *Materials* **2012**, *5*, 1084.
26. Arkles, B. Silane Coupling Agents: Connecting Across Boundaries v2.0, in: Gelest, Inc.: Morrisville, PA, USA, **2006**.
27. Park, S.-J.; Jin, J.-S. *J. Polym. Sci. Pol. Phys.* **2003**, *41*, 55.
28. Kulkarni, M. B.; Mahanwar, P. A. *J. Thermoplast. Compos. Mater.* **2013**, *27*, 1679.
29. Sanporean, C. G.; Donescu, D.; Vuluga, Z.; Christiansen, J. D.; Jensen, E. A.; Paven, H. *UPB Sci. Bull. Ser. B* **2013**, *75*, 3.
30. Fordiani, F.; Aubry, T.; Grohens, Y. *J. Appl. Polym. Sci.* **2009**, *114*, 4011.
31. Gupta, A. K.; Biswal, M.; Mohanty, S.; Nayak, K. *Fiber Polym.* **2014**, *15*, 994.
32. Kechaou, B.; Salvia, M.; Beaugiraud, B.; Juvé, D.; Fakhfakh, Z.; Treheux, D. *eXPRESS Polym. Lett.* **2010**, *4*, 171.
33. Zainal, Z.; Ismail, H. *Polym. Plast. Technol.* **2011**, *50*, 297.
34. Ficai, A.; Andronescu, E.; Ghitulica, C.; Voicu, G.; Trandafir, V.; Manzu, D.; Ficai, M.; Pall, S. *Mater. Plast.* **2009**, *46*, 11.